Earth and Planetary Science Letters 305 (2011) 83–91

Contents lists available at ScienceDirect

Earth and Planetary Science Letters

journal homepage: www.elsevier.com/locate/epsl

Modulation of the Southern Ocean cadmium isotope signature by ocean circulation and primary productivity

W. Abouchami [a,*], S.J.G. Galer [a], H.J.W. de Baar [b], A.C. Alderkamp [c], R. Middag [b], P. Laan [b], H. Feldmann [a], M.O. Andreae [a]

[a] Max Planck Institute for Chemistry, P.O. Box 3060, 55020 Mainz, Germany
[b] Royal Netherlands Institute for Sea Research, P.O. Box 59, 1790 AB Den Burg, The Netherlands
[c] Stanford University, Department of Environmental Earth System Science, Stanford, CA 94305-4216, USA

ARTICLE INFO

Article history:
Received 11 November 2010
Received in revised form 16 February 2011
Accepted 25 February 2011
Available online 2 April 2011

Editor: P. DeMenocal

Keywords:
Southern Ocean
cadmium isotopes
biogeochemical cycle
biological productivity proxy

ABSTRACT

The High Nutrient Low Chlorophyll (HNLC) Southern Ocean plays a key role in regulating the biological pump and the global carbon cycle. Here we examine the efficacy of stable cadmium (Cd) isotope fractionation for detecting differences in biological productivity between regions. Our results show strong meridional Cd isotope and concentration gradients modulated by the Antarctic Fronts, with a clear biogeochemical divide located near 56°S. The coincidence of the Cd isotope divide with the Southern Boundary of the Antarctic Circumpolar Current (ACC),together with evidence for northward advection of the Cd signal in the ACC, demonstrate that Cd isotopes trace surface ocean circulation regimes. The relationships between Cd isotope ratios and concentrations display two negative correlations, separating the ACC and Weddell Gyre into two distinct Cd isoscapes. These arrays are consistent with Rayleigh fractionation and imply a doubling of the isotope effect due to biological consumption of Cd during water transport from the Weddell Gyre into the ACC. The increase in magnitude of Cd isotope fractionation can be accounted for by differences in the phytoplankton biomass, community composition, and their physiological uptake mechanisms in the Weddell Gyre and ACC, thus linking Cd isotope fractionation to primary production and the global carbon cycle.

1. Introduction

The availability of trace nutrients, in particular iron, limits oceanic biological productivity in high nutrient low chlorophyll (HNLC) regions and hence impacts on the global carbon cycle (Boyd et al., 2005; De Baar et al., 1995; Martin et al., 1990). This is particularly so in regions remote from aeolian dust inputs which act as a source of trace nutrients to the oceans. The Southern Ocean is the largest HNLC region, where biomass and primary production are paradoxically relatively low despite the large inventory of major nutrients (nitrate, phosphate and silicate) available for phytoplankton growth (Holm-Hansen et al., 1977; Nelson and Smith, 1991). Paleoceanographic and box-model studies suggest that the nutrient status of the Southern Ocean might have been different in the past, affecting the efficiency of the biological pump in sequestering atmospheric CO_2 (Joos et al., 1991; Sigman and Boyle, 2000). Here we investigate the micronutrient cadmium (Cd) and, specifically, its stable isotope fractionation, as a novel proxy for ocean biological productivity in the Southern Ocean.

The biogeochemical cycle of cadmium in the oceans is relatively well-known with a distribution in seawater similar to that of phosphate (Boyle et al., 1976; Bruland, 1992). Surface waters are depleted in Cd due to removal by marine phytoplankton, which upon regeneration via organic matter decomposition and re-mineralization contribute to Cd enrichment in deep waters. The global oceanic correlation between Cd and PO_4 has been used alongside Cd/Ca ratios in foraminifera to reconstruct past changes in ocean circulation and nutrient distributions (Boyle, 1988). The discovery that Cd can substitute for zinc (Zn) in carbonic anhydrase – a vital enzyme involved in the photosynthetic acquisition of inorganic carbon by some marine diatoms – has established a biochemical function of Cd, linking directly the global marine cycles of cadmium and carbon (Lane et al., 2005; Price and Morel, 1990; Xu et al., 2008). Laboratory and field studies show that biological uptake of Cd from surface waters is related to its utilization by carbonic anhydrase and varies with dissolved CO_2 and Zn concentrations (Cullen et al., 1999).

In contrast, studies of marine stable Cd isotope fractionation are still in an early stage. The limited Cd isotope datasets thus far appear to indicate a biologically-mediated Cd isotope fractionation in the oceans (Lacan et al., 2006; Ripperger et al., 2007; Schmitt et al., 2009a). This "biological" effect is illustrated by a Cd isotope offset between surface waters (isotopically "heavy") and deep waters, which have more uniform compositions.

Here we show that stable Cd isotopes in surface waters track differences in biological productivity in the Southern Ocean and

* Corresponding author. Tel.: +49 6131 305 260; fax: +49 6131 371 051.
E-mail address: wafa.abouchami@mpic.de (W. Abouchami).

0012-821X/$ – see front matter © 2011 Elsevier B.V. All rights reserved.
doi:10.1016/j.epsl.2011.02.044

delimit two distinct biogeochemical oceanic provinces — the Antarctic Circumpolar Current (ACC) and the Weddell Gyre (Fig. 1). These first insights into the cycling and fractionation of Cd isotopes in the Southern Ocean emphasize their potential as a proxy for studies of present conditions and past changes in biological productivity.

2. The Southern Ocean

The Southern Ocean is dominated by the wind-driven Antarctic Circumpolar Current, which goes around Antarctica connecting the world oceans. With an eastward transport of ~150 Sv ($1\ \mathrm{Sv} = 10^6\ \mathrm{m^3\ s^{-1}}$) (Mazloff et al., 2010), the ACC is the largest ocean current, and thus a critical component of the global ocean circulation. Within the ACC, three fronts separate distinct water mass regimes (Orsi et al., 1995). Upwelling of Circumpolar Deep Water (CDW) in the Southern Ocean brings nutrient-rich waters to the surface which spread northwards in the surface Ekman layer across the Antarctic Polar Front (APF), towards the Polar Frontal Zone (PFZ) (Fig. 1a). Here it sinks to form Antarctic Intermediate Water (AAIW and then flows across the Subantarctic Front (SAF) into the Subantarctic Zone (SAZ) limited to the North by the Subtropical Front (STF), the northern extent of Subantarctic Surface Water (SASW). Some of the cold nutrient-rich water is "subducted" into the deep ocean interior

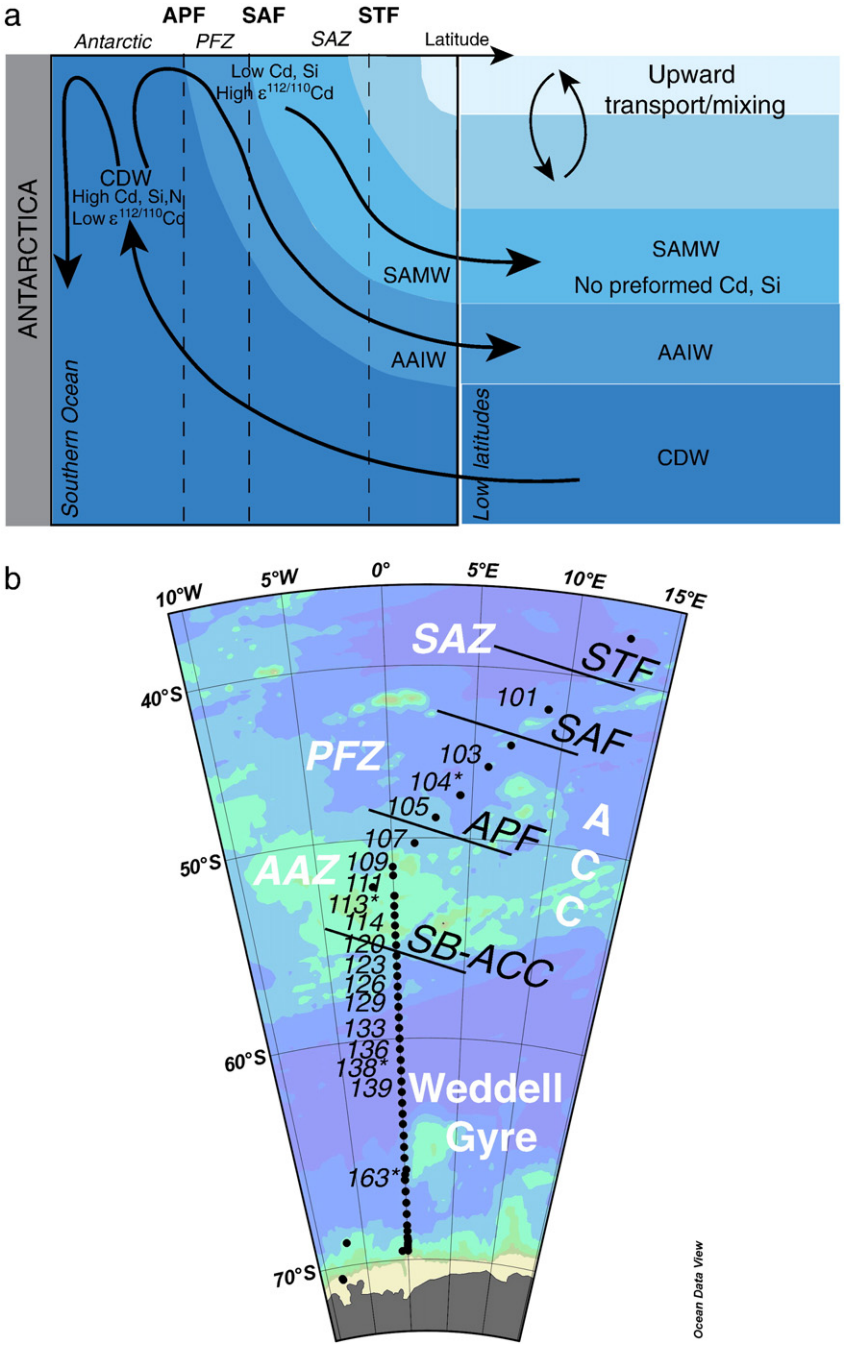

Fig. 1. (a) Schematic pattern of Southern Ocean circulation (modified after Sarmiento et al., 2004). Cd-rich Circumpolar Deep Water (CPDW) upwells to the surface in the Southern Ocean and spreads to the north across the Antarctic Polar Front (APF), the northern boundary of the Antarctic, into the Polar Frontal Zone (PFZ). It then sinks to form Antarctic Intermediate Water (AAIW), and then across the Subantarctic Front (SAF) into the Subantarctic Zone (SAZ) limited to the North by the Subtropical Front (STF). (b) Sampling locations during ANTXXIV/3 cruise showing the position of the Antarctic fronts and the different zones (Orsi et al., 1995). APF: Antarctic Polar Front, SB-ACC: Southern Boundary of the Antarctic Circumpolar Current; SAF: Sub Antarctic Front, AAZ: Antarctic Zone; PFZ: Polar Frontal Zone; SAZ: Subantarctic Zone. The map was produced with Ocean Dataview software (Schlitzer, 2009). (*) Stations sampled with ultraclean Titan frame (de Baar et al., 2008).

and contributes to the formation of Antarctic Bottom Water (AABW). The Southern Boundary of the ACC (SB-ACC) separates the ACC from the regime of the Weddell Gyre and corresponds to the location where the Upper Circumpolar Deep Water (UCDW) signal is no longer discernible due to shoaling and entrainment in the surface mixed layer (Orsi et al., 1995).

Biological productivity in the Southern Ocean is limited by availability of iron (De Baar et al., 1995; Martin et al., 1990) and light (De Baar et al., 2005; Mitchell et al., 1991; Sunda and Huntsman, 1997), as well as zooplankton grazing (Cullen, 1991). Seasonal relief occurs during phytoplankton blooms, with a predominance of diatoms supported by the high dissolved silica concentrations of Southern Ocean waters. Enhanced biological production has been shown to occur in relation to the Southern Ocean fronts (De Baar et al., 1995) and, recently, related to upwelling driven by interaction of the ACC with sea-floor topography (Sokolov and Rintoul, 2007).

3. Sampling and methods

Surface seawater samples were collected during the Geotraces ANT XXIV/3 expedition cruise (Fig. 1b) on board the German RV Polarstern (February 10 to April 16, 2008, austral late summer–early autumn, Cape Town, South Africa-Punta Arenas, Chile). Twelve surface water samples were collected at high spatial resolution between 41°S and 61°S, between two and five meters depth, during underway sampling using an IFISH torpedo sampler with an all-Teflon pump. In addition, four vertical profiles were sampled using the ultra-clean Titan Frame (De Baar et al., 2008), the surface data of which (depths in Table 1) are presented here to complement the surface transect. Samples were filtered on board in a class 100 clean room environment through 0.2 μm filter capsules (Sartobran-300, Sartorius) under slight nitrogen pressure and collected into acid-cleaned Nalgene high density polyethylene (HDPE) bottles and canisters. Sampled were acidified onboard to pH = 2 with 12 N HCl (Baseline, Seastar).

On return, samples of approximately one litre were weighed and spiked with an optimal amount of $^{106}Cd-^{108}Cd$ double spike – see Schmitt et al. (2009b) for details – and left to equilibrate for 24 h. Chemical separation and purification of the cadmium fraction from seawater samples was performed in two steps. The first column consists of a FEP separation funnel reservoir containing 2 ml of pre-cleaned BioRad AG1-X8 anion exchange resin in Cl^- form. The sample was acidified to pH = 1 by addition of high-purity 12 N HCl (Baseline Seastar) and loaded into the FEP reservoir. For a seawater matrix at this pH, the Cd partition coefficient onto the resin lies above 10^3 (Korkisch, 1989). The flow rate was adjusted to 1 ml/min, or less, by letting the effluent pass through a 10-mm section of 0.025 mm (0.001 in.)-bore PEEK tubing. After the sample had washed through, the resin was rinsed with 1 N HCl and, subsequently, Cd was eluted using 0.25 M HNO_3. This fraction was dried down and converted into bromide form. The secondary columns are home-made from 9.5 mm (3/8 in.) 4:1 shrink-fit Teflon filled with anion exchange resin (column: 100 μl AG1-X8 resin, 100–200 mesh). The Cd fraction was purified using HNO_3-HBr mixtures, as has been described elsewhere (Lugmair and Galer, 1992; Schmitt et al., 2009b).

Cadmium recovery was assessed by doping a “Cd-free” seawater (which had undergone Cd pre-extraction) with a known amount of JMC-Cd standard and processing this sample through the chemical procedure described above. The eluted Cd fraction was spiked after chemistry to obtain the recovery, which was found to be 96%. The total procedural Cd blank for our seawater protocol was 0.13 pmol (15 pg), a significant reduction compared to that in our previous studies on rocks and minerals (see Schmitt et al., 2009a,b).

Measurements of Cd isotopic compositions were performed by Thermal Ionization Mass Spectrometry (TIMS) on a ThermoFisher Triton instrument at the MPI for Chemistry (see Schmitt et al., 2009a,b). Isotope dilution Cd concentrations were derived from the isotopic composition run. The data are reported relative to our in-house JMC-Mainz standard which yielded a value of $^{110}Cd/^{112}Cd$ of 0.520083 ± 4 (2SD, N = 22) for 100 ng loads during the period of analysis (July 2009–March 2010) (Fig. 2a). In order to ease inter-laboratory comparison, the NIST SRM-3108 Cd standard was measured and has now been adopted by several laboratories as the "zero delta" isotope reference for cadmium (Abouchami et al., 2010b). Our measured $^{110}Cd/^{112}Cd$ for NIST SRM-3108 is 0.520121 ± 4 (2SD, N = 12) (Fig. 2a).

The long-term external reproducibility on $^{110}Cd/^{112}Cd$ for both standards analysed here is ±8 ppm (0.04 εCd/u), a significant improvement over previous double-spike Cd data reported by Schmitt et al. (2009b) (±14 ppm, 0.07εCd/u) and Ripperger et al. (2007) (±60 ppm, 0.3εCd/u). The external reproducibility based on duplicate seawater analyses is ±0.15ε units (±8 ppm/u) (see Fig. 2b), a factor of two larger than that for the standards, which is consistent with the smaller quantities of seawater Cd analysed.

The seawater Cd isotope data are expressed as $\varepsilon^{112/110}Cd$ defined by: $\varepsilon^{112/110}Cd_{sample} = ([^{110}Cd/^{112}Cd]_{standard}/[^{110}Cd/^{112}Cd]_{sample} - 1) \times 10^4$. Positive values of $\varepsilon^{112/110}Cd$ reflect enrichment in heavy Cd (^{112}Cd) relative to the light Cd (^{110}Cd) isotopes and vice-versa. The results are reported relative to both standards in Table 1, along with salinity, temperature and nutrient data plotted in Fig. 3 as a function of latitude.

4. Results and discussion

4.1. Cadmium gradients and Antarctic fronts

The distribution of Cd concentrations and $\varepsilon^{112/110}Cd$ values along the surface transect is shown in Fig. 4a as a function of latitude. These results show systematic and gradual changes in surface water Cd concentrations and $\varepsilon^{112/110}Cd$ with a strong meridional gradient. The isotope and elemental variations are antithetic: low Cd concentrations are associated with heavy Cd isotopic compositions (i.e. high $\varepsilon^{112/110}Cd$) and vice-versa. In the Weddell Gyre, Cd concentrations increase northward from 0.3 to 0.5 nmol kg^{-1}, while $\varepsilon^{112/110}Cd$ values decrease smoothly from +2.5 to +2.0. This trend is entirely reversed in the ACC: after a maximum in Cd at ca. 55°S near the SB-ACC, Cd concentrations decrease continuously across the APF, reaching a minimum of 0.04 nmol kg^{-1} in the SAZ, south of the SAF. The gradual depletion of Cd along the northward flow of circumpolar waters is accompanied by a concomitant increase in $\varepsilon^{112/110}Cd$ with the highest value of +5 observed in the PFZ, north of the APF. Most importantly, these changes occur systematically with respect to the location of the Antarctic fronts demonstrating that Cd isotopes and concentrations respond to differences in the surface ocean circulation.

We interpret the meridional gradient in Cd isotopes and concentrations in the Southern Ocean as reflecting the progressive depletion of Cd in nutrient-rich Antarctic waters induced by biological uptake during the northward transport of CDW across the APF into the PFZ and SAZ. The concentration gradient, previously documented at lower resolution (Löscher et al., 1998), is associated with similar changes in the nutrients phosphate, silica and nitrate, which all decrease northward along the transect with noticeably greater depletion for Cd than PO_4 in the northernmost waters (Fig. 3c, d, and e). As a result, these nutrients (N, PO_4 and Si) show tight correlations with both Cd concentrations and isotopic compositions (not shown) to be discussed elsewhere. These trends suggest that nutrient delivery to the SAZ and PFZ occurs predominantly via northward Ekman transport from the region south of the APF, where cold nutrient-rich waters upwell to the surface of the Southern Ocean (Orsi et al., 1995) (Fig. 1a).

Since the Cd isotopic composition tracks the northward changes in Cd concentration remarkably well, the relationships between these two parameters can be used to gain insights into both physical and biological processes operating in the Southern Ocean. The reversal in

Table 1
Cadmium concentration and isotopic composition along with CTD and nutrient data of surface waters sampled along the Zero Meridian (Polarstern ANTXXIV/III cruise, 10 February−16 April 2008, Cape Town–Punta Arenas). Sample depths correspond to average upper surface 2–5 m, except where stated otherwise. Cd isotope compositions are expressed as $\varepsilon^{112/110}Cd_{sample} = [^{110}Cd/^{112}Cd]_{standard}/[^{110}Cd/^{112}Cd]_{sample}$ -1)x10^4, relative to our in-house Cd standard Johnson Matthey Cd (JMC-Mainz) ($[^{110}Cd/^{112}Cd]_{JMC\text{-}Mainz} = 0.520083 \pm 4$ (2SD, N = 22)) and, NIST SRM-3108 Cd ($[^{110}Cd/^{112}Cd]_{NIST} = 0.520121 \pm 4$ (2SD, N = 12)). Cd concentrations by isotope dilution were derived from the fractionation-corrected $^{106}Cd/^{112}Cd$ ratios. "PS71-101": Polarstern expedition "71", station "101"; "1" or "2", cast number. All samples collected using the IronFISH except those marked (*) collected with ultra-clean CTD Titan frame; (§) GO-FLO bottles. $Nutrient values from most nearby station hydrocasts. [a]Weighed mean of two runs, [b]duplicate dissolution.

	Station	Date	Depth (m)	Latitude	Longitude	Salinity (‰)	Temperature (°C)	PO_4 (μmol kg^{-1})	Si (μmol kg^{-1})	NOx (μmol kg^{-1})	NO_2 (μmol kg^{-1})	NO_3 (μmol kg^{-1})	Si* (μmol kg^{-1})	Cd (nmol kg^{-1})	$^{110}Cd/^{112}Cd$	$\varepsilon^{112/110}Cd$ JMC-Mainz	$\varepsilon^{112/110}Cd$ NIST SRM-3108	2σ	Cd/PO_4	NO_3/Cd	NO_3/PO_4	Si/Cd
Sub-Antarctic ACC	*PS71-101-2*	13/02/2008		42° 20.33′ S	8° 59.61′ E	34.02	10.99	1.04	0.49	14.35	0.19	14.16	−13.7	0.036	0.519949 ± 58	2.59	3.32	1.12	0.035	390	13.7	13.5
PFZ	*PS71-103-1*	16/02/2008		45° 59.97′ S	5° 52.87′ E	33.75	7.84	1.21	0.88	17.11	0.16	16.95	−16.1	0.155	0.519863 ± 17	4.23	4.96	0.32	0.128	110	14.0	5.7
PFZ	PS71-104-2 *a	16/02/2008	14.5	47° 40.31′ S	4° 17.36′ E	33.73	6.47	1.35	1.86	19.50	0.27	19.23	−17.4	0.260	0.519914 ± 10	3.25	3.98	0.20	0.193	74	14.3	7.2
PFZ	PS71-104-2 *b	16/02/2008				33.73	6.47	1.35	1.86	19.50	0.27	19.23	−17.4	0.255	0.519920 ± 22	3.14	3.88	0.41	0.189	75	14.3	7.3
PFZ	PS71-105 $	17/02/2008		48°2.03′ S-48°3.04′ S	3° 49.52′ E - 3° 48.33′ E	33.71	6.28	1.40	1.89	20.12	0.27	19.85	−18.0	0.249	0.519891 ± 10	3.70	4.43	0.20	0.178	80	14.2	7.6
PFZ	*PS71-107*	18/02/2008		50°15.73′ S	1°25.95′ E	33.76	3.18	1.51	12.31	23.41	0.32	23.09	−10.8	0.388	0.519957 ± 11	2.43	3.16	0.22	0.256	60	15.2	31.7
AAZ	PS71-109	19/02/2008		51°39.44′ S-51°40.59′ S	0° 0.27′ E - 0° 0.31′ E	33.70	2.70	1.56	15.68	24.36	0.33	24.03	−8.3	0.415	0.519965 ± 10	2.27	3.00	0.19	0.266	58	15.4	37.8
AAZ	PS71-111	19/02/2008		52°9.58′ S-52°10.22′ S	0° 31.50′ W - 0° 33.12′ W	33.69	2.30	1.69	23.27	25.60	0.35	25.26	−2.0	0.513	0.519984 ± 6	1.91	2.64	0.11	0.303	49	14.9	45.4
AAZ	PS71-113-1 *	20/02/2008	9.9	52° 59.92′ S	0° 0.81′ E	33.79	1.27	1.73	35.26	26.04	0.33	25.71	9.5	*0.554*	0.519991 ± 13	1.78	2.51	0.25	0.320	46	14.9	63.6
AAZ	PS71-114	20/02/2008		53°10.19′ S-53°11.55′ S	0° 0.017′ E - 0° 0.0299′ E	33.76	1.42	1.80	34.31	26.80	0.34	26.46	7.8	0.527	0.519991 ± 6	1.78	2.51	0.12	0.293	50	14.7	65.1
AAZ	PS71-117	21/02/2008		54° 18.86′ S-54° 19.64′ S	0° 1.098′ E - 0° 1.163′ E	33.82	0.98	1.84	44.32	27.29	0.30	26.99	17.3	0.620	0.520007 ± 8	1.46	2.19	0.15	0.337	44	14.7	71.5
SB ACC	PS71-120	21/02/2008		55° 13.71′ S-55° 14.36′ S	0° 0.0112′ W - 0° 0.0194′ W	33.78	0.81	1.80	50.26	26.36	0.27	26.09	24.2	0.525	0.519998 ± 7	1.64	2.37	0.14	0.291	50	14.5	95.7
Weddell Gyre	PS71-123	22/02/2008		56° 17.78′ S-56° 18.41′ S	0° 0.029′ W - 0° 0.0065′ E	33.96	0.67	1.84	63.77	26.67	0.25	26.42	37.4	0.509	0.520007 ± 6	1.47	2.20	0.12	0.276	52	14.3	125.3
	PS71-126	23/02/2008		57° 11.97′ S-57° 13.04′ S	0° 0.007′ W - 0° 0.015′ W	34.08	0.64	1.87	64.78	27.31	0.28	27.04	37.7	0.525	0.520012 ± 7	1.36	2.09	0.12	0.282	51	14.5	123.4
	PS71-129 $	24/02/2008		58° 11.65′ S-58° 12.19′ S	0° 0.0108′ W - 0° 0.005′ E	34.03	0.34	1.84	67.09	26.41	0.26	26.15	40.9	0.459	0.519999 ± 8	1.62	2.35	0.14	0.250	57	14.2	146.2
	PS71-133	24/02/2008		59° 0.003′ S-58° 59.99′ S	0° 0.037′ E - 0° 0.0130′ E	33.98	0.19	1.84	62.69	26.23	0.31	25.92	36.8	0.431	0.519997 ± 8	1.65	2.38	0.16	0.234	60	14.1	145.5
	PS71-136	26/02/2008		60° 14.38′ S-60° 14.94′ S	0° 0.013′ W - 0° 0.0076′ W	33.91	0.11	1.76	62.13	25.22	0.21	25.01	37.1	0.392	0.519993 ± 6	1.74	2.47	0.12	0.222	64	14.2	158.5
	PS71-138-1 *a	26/02/2008	24.8	61° 0.04′ S	0° 0.44′ W	33.91	0.19	1.63	57.04	22.94	0.17	22.77	34.3	0.334	0.519948 ± 4	2.59	3.32	0.27	0.205	68	14.0	170.8
	PS71-139	26/02/2008		61° 8.66′ S-61° 9.49′ S	0° 0.006′ W - 0° 0.001′ W	33.91	0.40	1.69	57.62	23.49	0.16	23.33	34.3	0.314	0.519985 ± 12	1.89	2.62	0.22	0.186	74	13.8	183.5
	PS71-163-1 *	09/03/2008	8.8	67° 0.04′ S	0° 0.12′ E	33.97	-0.75	1.71	62.60	26.38	0.23	26.15	36.5	0.460	0.519968 ± 8	2.22	2.95	0.16	0.269	57	15.3	136.1

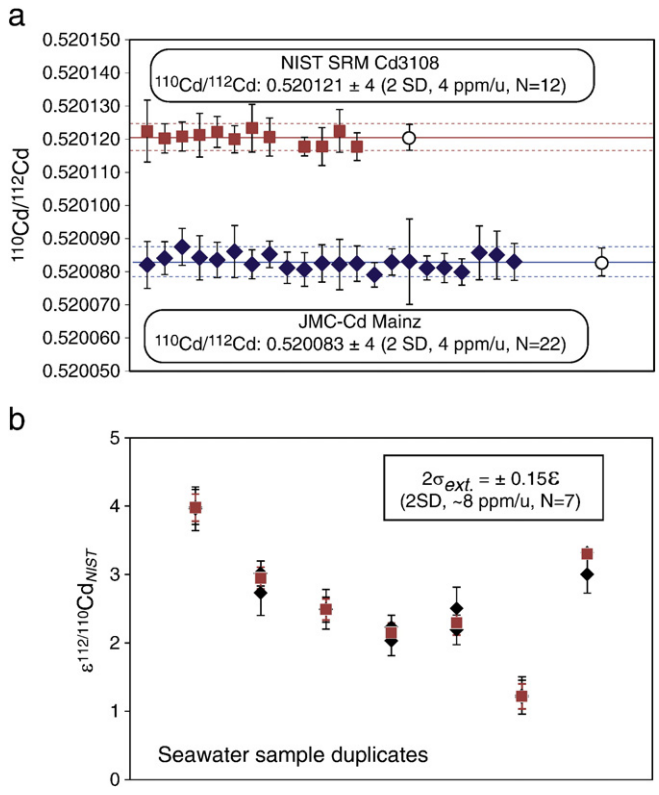

Fig. 2. External reproducibility of (a) $^{110}Cd/^{112}Cd$ ratios based upon the standards JMC-Mainz Cd (blue, diamonds) and NIST SRM 3108 (red, squares) treated as unknowns using the double-spike TIMS method on 100 ng-size loads(analysis period: July 2009–March 2010), open circles correspond to the average values; (b), $\varepsilon^{112/110}Cd$ of seawater duplicate measurements, with individual analyses shown as solid diamonds and weighed mean as squares, to be published elsewhere(see Abouchami et al., 2009, 2010a). For the standards (a), the long-term reproducibility is ±8 ppm (2SD), while that of seawater (b) is ±15 ppm (2SD), consistent with the smaller quantities of cadmium available.

trend of the Cd isotope/elemental signal in surface waters near the SB-ACC (Fig. 4a) is illustrated in Fig. 4b where $\varepsilon 112/^{110}Cd$ values are plotted against the natural logarithm of the Cd concentration. The gradual changes observed in Fig. 4a translate into two well-defined negative correlations (Figs. 4b and c) that separate the ACC waters from those of the Weddell Gyre. These two lines are resolved outside analytical errors, as is shown in Fig. 4c. The single sample collected in the SAZ has the lowest Cd concentration measured (0.04 nmol kg^{-1}) and falls well below the ACC and Weddell Gyre arrays. Two samples from the Weddell Gyre fall along the ACC array — the cause of this offset will be discussed later.

These linear arrays, along with the strong meridional gradients shown in Fig. 4a, identify two distinct Cd isoscapes in the Southern Ocean – the ACC and the Weddell Gyre – and possibly a third Cd isotope domain represented by the SAZ. The Cd isotope data delimit a clear biogeochemical divide located at ca. 56°S (Fig. 4a), coinciding remarkably well with the SB-ACC — the oceanographic boundary separating the ACC and Weddell Gyre (Orsi et al., 1995). The coincidence of the Cd isotope divide and a major oceanographic front provides compelling evidence for a link between the seawater Cd isotope signal and ocean circulation. Strengthening of Cd depletion and enrichment in "heavy" Cd towards northern latitudes along the ACC correlation (Fig. 4b) support advection of the Cd isotope signal northwards in the surface layer.

This interpretation agrees well with previous evidence based on surface nitrate concentration in the Southern Ocean (Sigman et al., 1999) and the distribution of Si* ($Si^* = [Si(OH)_4] - [NO_3^-]$), a proxy of nutrient availability for diatom growth (Sarmiento et al., 2004). The Cd concentration gradient mirrors remarkably that of PO_4, Si* and DIC along the Zero Meridian transect with a slight shift in the maxima (Fig. 6a). This shift reflects sequential and preferential removal by phytoplankton of silicate, followed by Cd and then PO_4. Note that the difference between the surface distribution of silicate and the "Redfield" nutrients phosphate and nitrate was first pointed out by Boyle and Edmond (1975).

As the Cd concentration decreases in the ACC, Si* becomes increasingly negative, reaching the lowest values in the SAZ. This "negative" Si* identifies Subantarctic Mode Water (SAMW) as a Cd-depleted water mass ([Cd] = 0.04 nmol kg^{-1}) resulting from progressive stripping out of Cd by marine phytoplankton along the northward water flow (Fig. 1a). This is also supported by the co-variation between Si* and $\varepsilon^{112/110}Cd$ values (not shown) in the ACC, suggesting that both Cd concentrations and isotopic compositions are diagnostic of biological productivity.

4.2. Cadmium isotopes: tracer of primary production

When the ACC and Weddell Gyre arrays are considered, the co-variations between Cd isotope ratios and concentrations could be interpreted in terms of binary mixing which would imply the involvement of three distinct components (Fig. 4b). The intersection of these two arrays indicates that they share a common component whose $\varepsilon^{112/110}Cd$ is inferred to be +2 and the Cd concentration 0.8 nmol kg^{-1}. These values correspond precisely to those measured for UCDW in vertical profiles from the Southern Ocean (Abouchami et al., 2009, 2010a) and, therefore, identify UCDW as the ultimate nutrient source for the low-latitude thermohaline circulation.

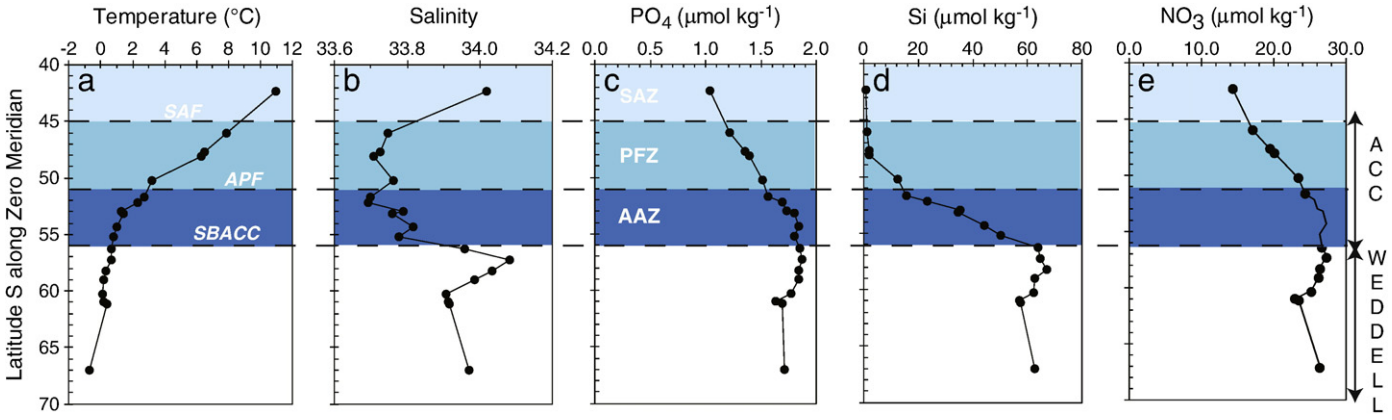

Fig. 3. Temperature (a), salinity (b) and nutrient data PO_4 (c); $Si(OH)_4$ (d); NO_3(e).

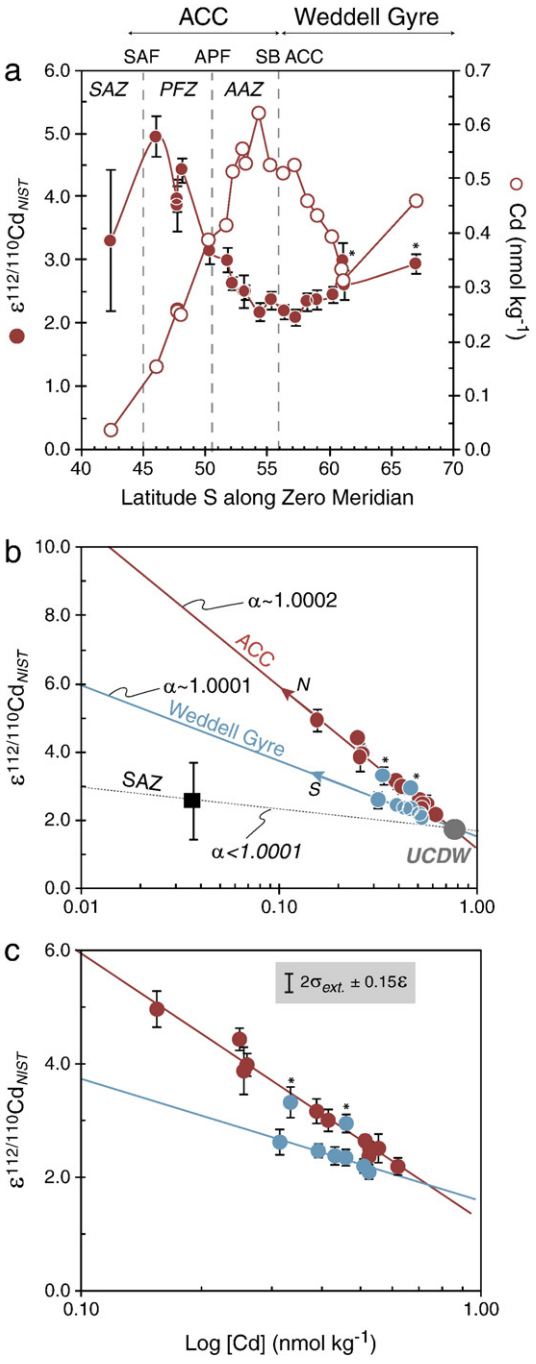

Fig. 4. (a) Latitudinal variations in seawater Cd isotope composition, expressed as $\varepsilon^{112/110}$Cd (solid symbol) and Cd concentration (open symbol) along Zero Meridian. Error bars on $\varepsilon^{112/110}$Cd are 2σ (95% confidence). The gradual and concomitant changes in Cd isotope composition and concentration across the APF reflect increasing Cd depletion and $\varepsilon^{112/110}$Cd of Antarctic waters northwards into the ACC. This gradient reflects upwelling of Cd-rich waters south of the APF which upon northward transport becomes Cd-depleted due to stripping out of Cd by phytoplankton. (b) Co-variations between $\varepsilon^{112/110}$Cd and [Cd] (nmol kg^{-1}) in Southern Ocean surface waters; (c) Enlarged version of (b). The negative correlations between $\varepsilon^{112/110}$Cd and [Cd] for the different zones (ACC, Weddell Gyre) of the Southern Ocean are consistent with closed-system Rayleigh fractionation. The slopes of the regression lines indicate a Cd fractionation factor $(\alpha-1)$ in the ACC twice that in the Weddell Gyre. The intercept and intersection of the two arrays is consistent with the composition of UCDW shown as a solid circle. The dotted line through the single sample from the Subantarctic Zone illustrates the possible existence of a third Cd isoscape. (*) Stations PS138 and PS163 within the Weddell Gyre fall along the ACC array (see text for explanation).

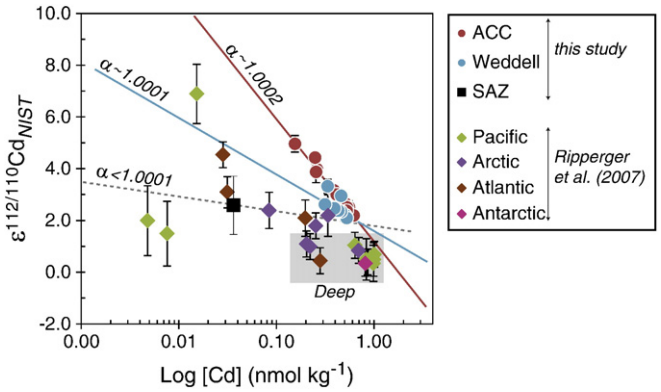

Fig. 5. Comparison of our Cd isotope data from the Southern Ocean with those from other ocean basins (excluding two samples) reported by Ripperger et al. (2007). All data have been expressed in $\varepsilon^{112/110}$Cd and re-normalized to the NIST SRM-3108 Cd standard. Note that our data are solely from surface waters whereas the data in Ripperger et al. (2007) are from vertical depth profiles and include deep water samples (grey shaded box).

In isotope-trace element ratio plots, binary mixing is characterized by hyperbolic relationships, which degenerate into straight lines when the denominators on both ordinates are the same. In $\varepsilon^{112/110}$Cd versus Si/Cd (Fig. 6b), the data display a curve rather than a straight line, indicating that simple binary mixing of water masses with distinct Si/Cd ratios cannot account alone for the co-variations observed. Rather, the composition of the extreme end-members reflects the advected Cd isotope signal modified by variable extents of biological uptake of Cd in the ACC and Weddell Gyre.

The negative correlations in Fig. 4b are consistent with an apparent closed system Rayleigh fractionation (e.g. Mariotti et al., 1981), and thus effectively establish a direct link between Cd uptake by phytoplankton and Cd isotope fractionation in the Southern Ocean. Previous direct seawater measurements by Ripperger et al. (2007) have suggested a $^{112}Cd/^{110}Cd$ fractionation factor α in the range of 1.0001 to 1.0003. Comparison of both datasets in Fig. 5 (excluding their two most extreme points from the North Pacific) shows a broad, overall agreement. Note that the data of Ripperger et al. (2007) include deep waters (Fig. 5) while our data are solely from surface waters.

The fraction of nutrients that can be utilized by phytoplankton is highly dependent on biological uptake mechanisms, which should also affect the Cd isotope systematics. Biological processes are generally described in terms of kinetic isotope reactions, with preferential uptake of the lighter isotopic species by marine organisms due to the lower energy "costs" associated with breaking molecular bonds involving “light” atoms (Mariotti et al., 1981). This process results in a net fractionation between the substrate (seawater), which becomes “heavier”, and the “lighter” organic products (phytoplankton). Therefore, increased Cd consumption by marine organisms will tend to force the $\varepsilon^{112/110}$Cd of seawater towards more positive values and progressively so for the resulting organic matter.

Our results show that the “heaviest” Cd isotope signatures (high $\varepsilon^{112/110}$Cd) are found in surface waters in the PFZ, north of the APF, while the “lightest”(low $\varepsilon^{112/110}$Cd) occur near the SB-ACC. In addition, strengthening of the “biological” Cd isotope signal with latitude along the two arrays occurs northward, in the ACC, and southward, in the Weddell Gyre (Fig. 4b). This observation agrees with variations in phytoplankton biomass along the Zero Meridian transect inferred from ^{234}Th data and SeaWiFS chlorophyll distribution maps (Rutgers van der Loeff et al., 2011), direct Chlorophyll *a* (Chl *a*) measurements (Alderkamp et al., 2010), and CTD fluorescence data. The distribution of Chl *a* shown in Fig. 7a displays a very similar pattern to that of $\varepsilon^{112/110}$Cd values along the surface transect. The $\varepsilon^{112/110}$Cd maximum at 47°S coincides with a Chl *a* peak and is followed by a region of low $\varepsilon^{112/110}$Cd and correspondingly low Chl *a* concentrations between 54°and 59°S. The high $\varepsilon^{112/110}$Cd values found in the Weddell Gyre at 61°S (PS138) and

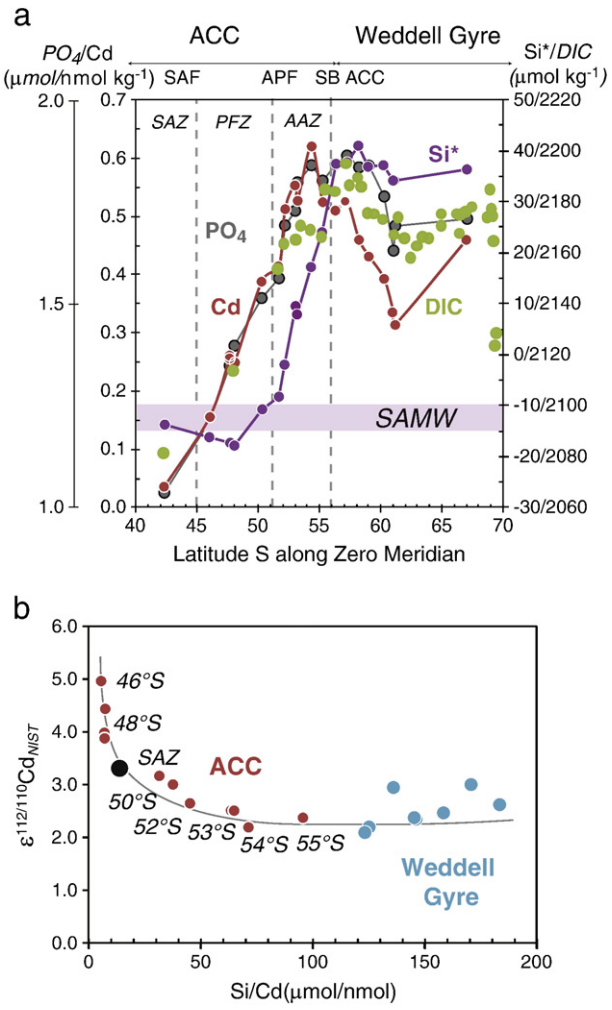

Fig. 6. (a) Variations of Cd, PO_4, DIC and Si* (Si* = $[Si(OH)_4]$–$[NO_3^-]$) (Sarmiento et al., 2004) as a function of latitude. South of the SAF, SAMW (Sub-Antarctic Mode Water) is identified as Cd-depleted (and Cd-heavy) water mass due to removal of Cd by phytoplankton as the water moves into the PFZ and across the APF (see also Fig. 1a). Note the greater depletion of Cd relative to PO_4 in the northernmost waters. (b) $\varepsilon^{112/110}$Cd versus Si/Cd. The data display a curve (drawn schematically) rather than the straight line that would be expected in the case of simple binary mixing of water masses.

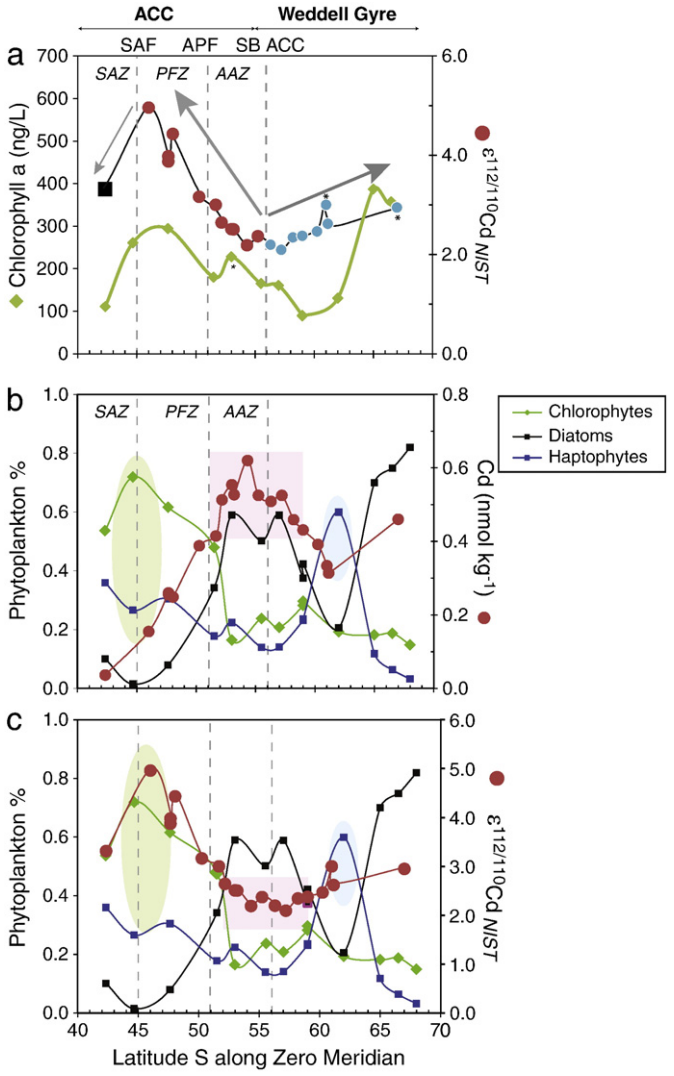

Fig. 7. (a) Variations of $\varepsilon^{112/110}$Cd and Chl *a* concentration as a function of latitude. Note the similarity of the two patterns indicating that Cd isotopes track phytoplankton biomass variation along the surface water transect. The arrows illustrate the direction of the increase in $\varepsilon^{112/110}$Cd along the arrays which occurs northward in the ACC and southward in the Weddell Gyre. (b) Relationships between Cd concentration and (c) $\varepsilon^{112/110}$Cd with the relative proportions of phytoplankton groups along the surface transect. Phytoplankton data from Alderkamp et al. (2010). (*) Stations PS138 and PS163 within the Weddell Gyre which fall along the ACC array (see text for explanation).

65°S(PS163) correspond to the samples that fall along the ACC array in Fig. 4a and match the peak in haptophytes (Fig. 6a). These values are consistent with reports of a phytoplankton bloom between 60°S and 65°S, earlier in the preceding season, from December 2007 to January 2008 period (Rutgers van der Loeff et al., 2011). Hence, the strength of the "biological" Cd isotope response to enhanced Cd utilization provides, in effect, a measure of oceanic biological productivity.

Quantitative constraints on Cd uptake and isotope fractionation can be extracted from the Rayleigh equation

$$\varepsilon^{112/110}\mathrm{Cd} = \varepsilon^{112/110}\mathrm{Cd}_{t=0} - \alpha \ln\{[\mathrm{Cd}]/[\mathrm{Cd}]_{t=0}\}.$$

Assuming a closed system with no new Cd input, the slope of the line in $\varepsilon^{112/110}$Cd versus $\ln\{[Cd]/[Cd]_{t=0}\}$ yields the Rayleigh fractionation factor α for $^{112}Cd/^{110}Cd$. Values for α calculated in Table 2 assume an initial [Cd] of 0.8 nmol kg^{-1} based on the intersection of the two lines in Fig. 4b. These α values imply that the "isotope effect" on $^{112}Cd/^{110}Cd$ due to biological Cd consumption is actually not constant within the Southern Ocean, but in fact is twice as high in the ACC ($\alpha = 1.0002$) than in the Weddell Gyre ($\alpha = 1.0001$) (Fig. 4b, Table 2).

Estimates of the fraction of Cd consumed by phytoplankton along the northward flow of CPW indicate that by the time Antarctic surface waters reach the SAF, up to 80% of the seawater Cd pool has been consumed by marine organisms. This biological Cd consumption leaves behind a seawater with a "heavy" Cd isotope signature ($\varepsilon^{112/110}Cd = +5$) and a Cd concentration of 0.15 nmol kg^{-1}, as observed at 47°S (Fig. 4a). By comparison, the maximum Cd utilization is about 60% in the Weddell

Table 2
Linear least-square regression parameters of $\varepsilon^{112/110}$Cd versus ln [Cd] using the Williamson/Minster method.

	ACC	Weddell Gyre
Slope	-2.12 ± 0.11	-1.031 ± 0.13
α	1.00021	1.00010
Intercept: $\varepsilon^{112/110}$Cd	1.16 ± 0.11	1.49 ± 0.12
N	11	6
χ^2 red.	0.07	0.05

Gyre, resulting in a "lighter" isotope signature ($\varepsilon^{112/110}Cd = +2.4$) and a higher Cd concentration of 0.3 nmol kg^{-1}.

4.3. Factors controlling Cd isotope fractionation in the Southern Ocean

In general, variation in the magnitude of biologically-mediated kinetic isotope fractionation may depend on the reaction rates, the concentrations of products and reactants, the environmental conditions, and the species of organisms in the case of metabolic transformations. Below, we discuss how these factors may affect isotope fractionation in the Southern Ocean.

Low iron availability and low light levels limit phytoplankton growth in the Southern Ocean (De Baar et al., 2005; Mitchell et al., 1991; Sunda and Huntsman, 1997). Chronic Fe limitation has also been proposed as an explanation for the "kink" observed in the global oceanic Cd – PO_4 correlation, thus linking the oceanic cycles of Cd and Fe (Cullen, 2006). Iron concentrations in surface waters are slightly lower in the Weddell Gyre (0.19 ± 0.1 nmol kg^{-1}) compared to those in the ACC (0.24 ± 0.08 nmol kg^{-1}) (Klunder et al., 2011) and could thus affect Cd uptake by phytoplankton, as shown in laboratory studies (Lane et al., 2009). In addition, light availability can severely limit phytoplankton crop size in regions of the Southern Ocean where the mixed layer is deeper than the euphotic zone (Mitchell et al., 1991; Sunda and Huntsman, 1997). Interpreting our data in the light of field observations and laboratory experiments is difficult, however, since the Cd isotope signal measured in our samples most likely integrates the history of phytoplankton growth and light levels over the previous season. The lower fractionation factor observed in the Weddell Gyre sector would appear, nonetheless, consistent with the low productivity of Fe-depleted oceanic regions and acclimation of Antarctic phytoplankton in a low-light climate (Morel and Price, 2003).

The lack of Cd isotope data on marine phytoplankton makes it difficult to assess the relationships between the magnitude of Cd isotope fractionation observed and phytoplankton species composition. So far, the only experimental data available are from freshwater phytoplankton cultures. These data indicate a fractionation factor α of 1.0003 for $^{112}Cd/^{110}Cd$ with a large uncertainty ($\varepsilon^{112/110}Cd$ offset of -3.2 ± 2.8; Lacan et al., 2006) and thus within the range of our results for the Southern Ocean.

Our data resolve clear differences in biological fractionation of Cd isotopes between the ACC and the Weddell Gyre that may well be consistent with phytoplankton species distribution in the Southern Ocean. Two lines of evidence support this interpretation.

First, a taxonomic study identified three phytoplankton groups (chlorophytes, diatoms, haptophytes) distributed in variable proportions along the transect (Alderkamp et al., 2010). The variation in Cd concentrations and isotopic compositions in seawater are a mirror image of the distribution of diatoms (Fig. 6b and c): Cd-rich waters with low $\varepsilon^{112/110}Cd$ are found at stations with a high diatom proportion. In contrast, Cd-depleted waters with comparatively higher $\varepsilon^{112/110}Cd$ in the ACC are associated predominantly with chlorophytes. These observations are consistent with variations in cellular Cd content of cultured marine phytoplankton (Finkel et al., 2007; Ho et al., 2003). We note the correspondence of the Cd isotope excursion at 61°S (Fig. 4b) with a peak of the haptophyte *Phaeocystis antarctica* (Alderkamp et al., 2010).

Second, the gradient in surface water Cd isotope composition and concentration correlates with changes in temperature (Figs. 3 and 4). This relation suggests that the biogeographic distribution of phytoplankton in the Southern Ocean might play a role in controlling Cd isotope fractionation. This would agree with both field and laboratory experiments on marine phytoplankton that have shown the importance of temperature in shifting ecotype abundance and growth (Ellwood et al., 2005; Johnson et al., 2006).

Culture experiments show that both phytoplankton growth and Cd uptake rate are affected by low concentrations of Zn (Sunda and Huntsman, 2000) and Fe (Lane et al., 2009; Sunda and Huntsman, 1997). This, in combination with some effect of irradiance levels (Finkel et al., 2007), results in a net increase of cellular Cd accumulation to compensate for the limiting conditions typical of HNLC regions. Sunda and Huntsman (1998) described two transport systems of Cd in marine diatoms — a low-Zn induced system, that is unidentified yet, and a Mn uptake system at high Zn concentration. The increase in magnitude of the Cd isotope fractionation factor from the Weddell Gyre into the ACC might reflect a shift in Cd transport channels of the respective algal communities under different sets of conditions. In support of this, low dissolved Mn concentrations (Middag et al., 2011) along with slightly lower Fe concentration (Klunder et al., 2011) have been related to the higher requirement of Mn by diatoms in the Weddell Gyre compared to that in the ACC.

Because the Mn uptake system increases as the Mn concentration decreases (Sunda and Huntsman, 1998), a shift from a predominant Cd uptake via Mn transporters in the Weddell Gyre to the low-Zn system in the ACC, would provide a plausible explanation for the observed doubling of the Cd isotope effect. This would also be consistent with the higher dissolved Zn concentrations seen in the Weddell Gyre compared to those in the ACC (Croot et al., 2011). Physiological mechanisms were also suggested to account for biological fractionation of Zn isotopes in laboratory cultures by John et al. (2008). Altogether, our results hint at a phytoplankton species dependent Cd isotope fractionation in the Southern Ocean, but this will need to be confirmed by experimental determination of the actual Cd fractionation factors from marine phytoplankton cultures.

5. Conclusions and perspectives

Our study identifies a distinct Cd isotope boundary separating two biogeochemical provinces in the Southern Ocean — the ACC and the Weddell Gyre. This subdivision is consistent with models that suggest contrasting roles for the Antarctic and Subantarctic zones in regulating the biological pump and the pCO_2 of the atmosphere (Marinov et al., 2006). The increase in the magnitude of Cd isotope fractionation, as a result of enhanced phytoplankton biomass and altered species composition in the Southern Ocean, demonstrates that Cd isotopes could potentially serve as a useful measure of biological productivity.

This novel proxy may have interesting applications in paleoceanography. In particular, Cd isotopes might provide some useful insights into the hypothesis that glacial–interglacial changes in atmospheric CO_2 concentrations are related to past changes in high-latitude nutrient inventories and biological productivity (see discussion in Sigman and Boyle, 2000). If, as suggested by our data, increased biological activity produces a "heavy" Cd isotope signature, then such a signal would be expected in the case of increased nutrient utilization and productivity during glacial times. The SB-ACC boundary has recently been suggested as a driving force for global carbon cycle changes (Anderson et al., 2009), and coincides with the Cd isotope divide identified here. Paleorecords of Cd isotopes combined with other proxy records (Cd/Ca, $\delta^{13}C$, $\delta^{15}N$, $^{231}Pa/^{230}Th$) in sedimentary archives along this boundary will help validate this hypothesis and constrain the role of the Southern Ocean in regulating the past biological pump.

Acknowledgments

This contribution would not have been possible without the concerted efforts of the crew of FS Polarstern, the whole scientific team of the ANTXXIV/3 cruise, and those who did not return. Thanks to J. van Ooijen for nutrient analyses, M. Rutgers van der Loeff for sharing his SeaWiFs analyses, and I. Raczek, J. Krey, S. Barth and J. Krause for laboratory assistance and Mak Saito for discussions and useful insight. Ed Boyle and an anonymous reviewer, as well as Editor

Peter de Menocal, are thanked for constructive comments, which helped improve the manuscript. This work was supported by a MPG fellowship to W.A.

References

Abouchami, W., Galer, S.J.G., Middag, R., De Baar, H.J.W., Andreae, M.O., Feldmann, H., Raczek, I., 2009. The Cd isotope signature of the Southern Ocean. Eos Trans. AGU Fall Meet. Suppl. 90, PP13A-1376.

Abouchami, W., Galer, S.J.G., Middag, R., De Baar, H.J.W., Andreae, M.O., Feldmann, H., Laan, P., Raczek, I., 2010a. Cd isotopes, a proxy for water mass and nutrient uptake in the Southern Ocean. EosTrans. AGUOcean Sci. Meet. Suppl. 91, CO13A-03.

Abouchami, W., Rehkämper, M., Galer, S.J.G., Horner, T.J., Xue, Z., Henderson, G.M., Wombacher, F., Schonbachler, M., Gault-Ringold, M., Stirling, C., 2010b. In search of a common reference standard for Cd isotopes. Geochim. Cosmochim. Acta 74, A2.

Alderkamp, A.C., De Baar, H.J.W., Visser, R.J.W., Arrigo, K.R., 2010. Can photoinhibition control phytoplankton abundance in deeply mixed water columns of the Southern Ocean? Limnol. Oceanogr. 55, 1248–1264.

Anderson, R.F., Ali, S., Bradtmiller, L.I., Nielsen, S.H.H., Fleisher, M.Q., Anderson, B.E., Burckle, L.H., 2009. Wind-driven upwelling in the Southern Ocean and the deglacial rise in atmospheric CO_2. Science 323, 1443–1448.

Boyd, P.W., Jickells, T., Law, C.S., Blain, S., Boyle, E.A., Buesseler, K.O., Coale, K.H., Cullen, J.J., de Baar, H.J.W., Follows, M., Harvey, M., Lancelot, C., Levasseur, M., Owens, N.P.J., Pollard, R., Rivkin, R.B., Sarmiento, J., Schoemann, V., Smetacek, V., Takeda, S., Tsuda, A., Turner, S., Watson, A.J., 2005. Mesoscale iron enrichment experiments 1993–2005: synthesis and future directions. Science 315, 612–617.

Boyle, E., 1988. Cadmium: chemical tracer of deepwater paleoceanography. Paleoceanography 3, 471–489.

Boyle, E., Edmond, J.M., 1975. Copper in surface waters south of New Zealand. Nature 253, 107–109.

Boyle, E., Sclater, F., Edmond, J.M., 1976. On the marine geochemistry of Cadmium. Nature 263, 42–44.

Bruland, K.W., 1992. Complexation of Cadmium by natural organic ligands in the Central North Pacific. Limnol. Oceanogr. 37, 1008–1017.

Croot, P.L., Baars, O., Streu, P., 2011. The distribution of dissolved Zinc in the Atlantic sector of the Southern Ocean. Deep Sea Res. Part II. doi:10.1016/j.dsr2.2010.10.041.

Cullen, J.T., 1991. Hypotheses to explain high nutrient conditions in the open sea. Limnol. Oceanogr. 36, 1579–1599.

Cullen, J.T., 2006. On the nonlinear relationship between dissolved Cadmium and Phosphate in the modern global ocean: could chronic iron limitation of phytoplankton growth cause the kink? Limnol. Oceanogr. 51, 1369–1380.

Cullen, J.T., Lane, T.W., Morel, F.M.M., Sherrell, R.M., 1999. Modulation of cadmium uptake in phytoplankton by seawater CO_2 concentration. Nature 402, 165–167.

De Baar, H.J.W., Boyd, P.W., Coale, K., Landry, H., Tsuda, M.R., Assmy, A.P., Bakker, D.C.E., Bozec, Y., Barber, R.T., Brzezinski, M.A., Buesseler, K.O., Boyé, M., Croot, P.L., Gervais, F., Gorbunov, M.Y., Harrison, P.J., Hiscock, W.T., Laan, P., Lancelot, C., Law, C., Levasseur, M., Marchetti, A., Millero, F.J., Nishioka, J., Nojiri, Y., van Oijen, T., Riebesell, U., Rijkenberg, M.J.A., Saito, H., Takeda, S., Timmermans, K.R., Veldhuis, M. J.W., Waite, A., Wong, C.S., 2005. Synthesis of iron fertilization experiments: from the iron age in the age of enlightenment. C09S16 In: Orr, J.C., Pantoja, S., Pörtner, H.-O. (Eds.), The Oceans in High CO_2 World, Special Issue of: J. Geophys. Res. (Oceans), 110, pp. 1–24. doi:10.1029/2004JC002601.

De Baar, H.J.W., Timmermans, K.R., Laan, P., De Porto, H.H.S., Ober, S., Blom, J.J., Bakker, M.C., Schilling, J., Sarthou, G., Smit, M.G., Klunder, M., 2008. Titan: a new facility for ultraclean sampling of trace elements and isotopes in the deep oceans in the international Geotraces program. Mar. Chem. 111, 4–21.

De Baar, H.J.W., DeJong, J.T.M., Bakker, D.C.E., Löscher, B.M., Veth, C., Bathmann, U., Smetacek, V., 1995. Importance of iron for plankton blooms and carbon dioxide drawdown in the Southern Ocean. Nature 373, 412–415.

Ellwood, M.J., Vanden Berg, S., Boye, M., Veldhuis, M., DeJong, J.T.M., De Baar, H.J.W., Croot, P.L., Kattner, G., 2005. Organic complexation of cobalt across the Antarctic Polar Front in the Southern Ocean. Mar. Freshwater Res. 56, 1069–1075.

Finkel, Z.V., Quigg, A.S., Chiampi, R.K., Schofield, O.E., Falkowski, P.G., 2007. Phylogenetic diversity in cadmium: phosphorus ratio regulation by marine phytoplankton. Limnol. Oceanogr. 52, 1131–1138.

Ho, T.Y., Quigg, A., Finkel, Z.V., Milligan, A.J., Wyman, K., Falkowski, P.G., Morel, F.M.M., 2003. The elemental composition of some marine phytoplankton. J. Phycol. 39, 1145–1159.

Holm-Hansen, O., El-Sayed, Z., Franceschini, G.A., Cuhel, L., 1977. Primary production and the factors controlling phytoplankton growth in the Southern Ocean. In: Llano, G.A. (Ed.), Adaptations within Antarctic ecosystems, Gulf, Houston, Texas, pp. 11–50.

John, S.E., Geis, R.W., Saito, M.A., Boyle, E.A., 2008. Zinc isotope fractionation during high-affinity and low-affinity zinc transport by the marine diatom Thalassiosira oceanica. Limnol. Oceanogr. 52, 2710–2714.

Johnson, Z.I., Zinser, E.R., Coe, A., McNulty, N.P., Woodward, E.M.S., Chisholm, S.W., 2006. Niche partitioning among Prochlorococcus ecotypes along ocean-scale environmental gradients. Science 311, 1737–1740.

Joos, F., Sarmiento, J., Siegenthaler, U., 1991. Estimates of the effect of Southern Ocean iron fertilization on atmospheric CO_2 concentrations. Nature 349, 772–775.

Klunder, M., Laan, P., Middag, R., De Baar, H.J.W., Van Ooijen, J.C., 2011. Dissolved Iron the Southern Ocean (Atlantic Sector). Deep Sea Res. II. doi:10.1016/j.dsr2.2010.10.042.

Korkisch, J., 1989. Handbook of Ion Exchange Resins: Their Application to Inorganic Analytical Chemistry, IV. CRC Press, Boca Raton. 352 pp.

Lacan, F., Francois, R., Ji, Y., Sherrell, R.M., 2006. Cadmium isotopic composition in the ocean. Geochim. Cosmochim. Acta 70, 5104–5118.

Lane, T.W., Saito, M.A., George, G.N., Pickering, I.J., Prince, R.C., Morel, F.M.M., 2005. Biochemistry: a cadmium enzyme from a marine diatom. Nature 435, 42-42.

Lane, E.S., Semeniuk, D.M., Strzepek, R.F., Cullen, J.T., Maldonado, M.T., 2009. Effects of iron limitation on intracellular cadmium of cultured phytoplankton: implications for surface dissolved cadmium to phosphate ratios. Mar. Chem. 115, 155–162.

Löscher, B.M., De Jong, J.T.M., De Baar, H.J.W., 1998. The distribution and preferential biological uptake of cadmium at 6W in the Southern Ocean. Mar. Chem. 62, 259–286.

Lugmair, G.W., Galer, S.J.G., 1992. Age and isotopic relationships among the angrites Lewis Cliff 86010 and Angra dos Reis. Geochim. Cosmochim. Acta 56, 1673–1694.

Marinov, I., Gnanadesikan, A., Toggweiler, J.R., Sarmiento, J.L., 2006. The Southern Ocean biogeochemical divide. Nature 441, 964–967.

Mariotti, A., Germon, J., Hubert, P., Kaiser, P., Letolle, R., Tardieux, A., Tardieux, P., 1981. Experimental determination of nitrogen kinetic isotope fractionation: some principles: illustration for the denitrification and nitrification processes. Plant Soil 62, 413–430.

Martin, J.H., Fitzwater, S.E., Gordon, R.M., 1990. Iron deficiency limits phytoplankton growth in Antarctic waters. Glob. Biogeochem. Cycles 4, 5–12.

Mazloff, M.R., Heimbach, P., Wunsch, C., 2010. An eddy-permitting Southern Ocean state estimate. J. Phys. Oceanogr. 40, 880–899.

Middag, R., De Baar, H.J.W., Laan, P., Cai, P.H., Van Ooijen, J.C., 2011. Dissolved Manganese in the Atlantic sector of the Southern Ocean. Deep Sea Res. Part II. doi:10.1016/j.dsr2.2010.10.043.

Mitchell, B.G., Brody, E.A., Holm-Hansen, O., McClain, C., Bishop, J., 1991. Light limitation of phytoplankton biomass and macronutrient utilization in the Southern Ocean. Limnol. Oceanogr. 36, 1662–1677.

Morel, F.M.M., Price, N.M., 2003. The biogeochemical cycles of trace metals in the oceans. Science 300, 944–947.

Nelson, D.M., Smith Jr., W.O., 1991. Sverdrup revisited: critical depths, maximum chlorophyll levels, and the control of Southern Ocean productivity by the irradiance-mixing regime. Limnol. Oceanogr. 36, 1650–1661.

Orsi, A.H., Whitworth, T., Nowlin, W.D., 1995. On the meridional extent and fronts of the Antarctic Circumpolar Current. Deep Sea Res. I 42, 641–673.

Price, N.M., Morel, F.M.M., 1990. Cadmium and cobalt substitution for zinc in a marine diatom. Nature 344, 658–660.

Ripperger, S., Rehkämper, M., Porcelli, D., Halliday, A.N., 2007. Cadmium isotope fractionation in seawater — a signature of biological activity. Earth Planet. Sci. Lett. 261, 670–684.

Rutgers van der Loeff, M., Cai, P., Stimac, I., Bracher, B., Middag, R., Klunder, M., Van Heuven, S., 2011. ^{234}Th in surface waters: distribution of particle export flux across the Antarctic Circumpolar Current and in the Weddell Sea during the GEOTRACES expedition ZERO and DRAKE. Deep Sea Res. II. doi:10.1016/j.dsr2.2011.02.004.

Sarmiento, J.L., Gruber, N., Brzezinski, M.A., Dunne, J.P., 2004. High-latitude controls of thermocline nutrients and low latitude biological productivity. Nature 427, 56–60.

Schlitzer, R., 2009. Ocean Data View. http://odv.awi.de.

Schmitt, A.D., Galer, S.J.G., Abouchami, W., 2009a. Mass-dependent cadmium isotopic variations in nature with emphasis on the marine environment. Earth Planet. Sci. Lett. 277, 262–272.

Schmitt, A.D., Galer, S.J.G., Abouchami, W., 2009b. High-precision cadmium stable isotope measurement by double spike thermal ionisation mass spectometry. J. Anal. At. Spectrom. 24, 1079–1088.

Sigman, D.M., Boyle, E.A., 2000. Glacial/interglacial variations in atmospheric carbon dioxide. Nature 407, 859–869.

Sigman, D.M., Altabet, M.A., McCorkle, D.C., Francois, R., Fischer, G., 1999. The δ^{15}N of nitrate in the Southern Ocean: consumption of nitrate in surface waters. Glob. Biogeochem. Cycles 13, 1149–1166.

Sokolov, S., Rintoul, S.R., 2007. On the relationship between fronts of the Antarctic Circumpolar Current and surface chlorophyll concentrations in the Southern Ocean. J. Geophys. Res. 112, C07030.

Sunda, W.G., Huntsman, S.A., 1997. Interrelated influence of iron, light and cell size on marine phytoplankton growth. Nature 390, 389–392.

Sunda, W.G., Huntsman, S.A., 1998. Processes regulating cellular metal accumulation and physiological effects: phytoplankton as model systems. Sci. Total Environ. 219, 165–181.

Sunda, W.G., Huntsman, S.A., 2000. Effect of Zn, Mn, and Fe on Cd accumulation in phytoplankton: implications for oceanic Cd cycling. Limnol. Oceanogr. 45, 1501–1516.

Xu, Y., Feng, L., Jeffrey, P.D., Shi, Y., Morel, F.M.M., 2008. Structure and metal exchange in the cadmium carbonic anhydrase of marine diatoms. Nature 452, 56–61.